Design of a Battery-Powered Induction Stove

by

Daniel J Weber

S.B., Massachusetts Institute of Technology, 2014

Submitted to the
Department of Electrical Engineering and Computer Science
in Partial Fulfillment of the Requirements for the Degree of

Master of Engineering in Electrical Engineering and Computer Science

at the

Massachusetts Institute of Technology

June 2015

Author: _____

Department of Electrical Engineering and Computer Science
May 22, 2015

Certified By: _____

Rich Fletcher, Thesis Supervisor
May 22, 2015

Accepted By: _____

Prof. Albert R. Meyer, Chairman, Masters of Engineering Thesis Committee

Design of a Battery-Powered Induction Stove

by
Daniel J Weber

Submitted to the Department of Electrical Engineering and Computer Science
on May 25, 2015, in partial fulfillment of the
requirements for the degree of
Master of Engineering in Electrical Engineering and Computer Science

Abstract

Many people in the developing areas of the world struggle to cook with stoves that emit hazardous fumes and contribute to green house gas emissions. Electric stoves would alleviate many of these issues, but significant barriers to adoption, most notably lack of reliable electric power, make current commercial options infeasible. However, a stove with an input power of 24V DC elegantly solves the issue of intermittent power by allowing car batteries to be used instead of a grid connection, while also allowing seamless integration with small scale solar installations and solar-based micro-grids. However, no existing commercial stoves nor academic research have attempted to create an induction stove powered from a low voltage DC source. This paper presents the design of a low voltage current-fed, full-bridge parallel resonant converter stove. The dynamics of this new topology are discussed in detail and simulations are provided to analyze the behavior. Additionally, a practical implementation of a 500W – 1 kW stove is described. This stove is the first of it's kind and represents a new contribution to both the field of induction cooking and the field of clean cooking solutions for the developing world.

Acknowledgments

I'd like to thank a number of people for their continued support. First and foremost, I'd like to thank the team at D-Lab. This work would not have been possible without help from my advisor, Rich Fletcher. Matt Okabue, Eder Guimarães dos Santos, and Giorgio Magalhães made significant contributions to the work presented here in their UROP programs. I'd also like to thank my family: my parents, without whom I wouldn't have had the opportunity to pursue my degree, and my sisters, who are both an inspiration to me. Finally, I'd like to thank my friends and my girlfriend, for keeping me going when times were difficult and who were always ready to rope up and go climbing when I needed a break!

Contents

List of Figures

Chapter One
Introduction

1.1 Motivation

Even in this modern era, nearly 150 years since the invention of the electric light bulb, many people in developing countries still use wood and kerosene for heating, cooking, and lighting [1]. Wood and kerosene are readily available, but have significant negative impacts on the health of those nearby, primarily through the emission of soot [2]. Burning these fuels also have a negative climate impact by releasing a significant amount of green house gases [1]. These technologies also operate at a very low efficiency, with only a small amount of the stored chemical energy being converted into heat for cooking or light for working.

This project focuses on improving cooking for those in developing countries. There has been a large body of work established already in this field. Several universities including MIT have labs devoted to improving cooking in these environments. There is also an ISO standard that has been established to provide a rigorous means of comparison between cooking technologies [3]. However, most of the focus in these labs has been on improving the traditional wood fire, improving charcoal formulations, or similar advances that still make use of the same fundamental fuel sources. Instead, this project will focus on electric heating as a clean alternative. Electric heating emits no soot or green house gases. Electric heating also allows fine heat control that wood and fossil fuel burning stove do not. Furthermore, electric heating can be significantly more efficient, with a much higher percent of energy going into heating the food

than is achievable by traditional methods [4].

1.2 Previous Work

This project will focus on using electric power for cooking. There are two common ways for electric stoves to function. The first method is driving current through a resistive element. This produces ohmic heating and the thermal energy is transferred to the pot or pan through thermal conduction. This was deemed infeasible due to low efficiency, since only 60% of power consumed may be used to heat the pot containing the food or water [4]. The importance of higher efficiency, especially with regard to electric power, will be discussed more thoroughly later.

The second method, which we will examine more completely as the focus for this proposal, is the use of induction to heat the pot directly. In an induction stove, the stove produces a strong, time varying magnetic field. If the pot, made of an appropriately conductive material, is placed in the field, currents will flow in the pot to generate a magnetic field to oppose the exciting field according to Maxwell's equations. These induced current in the pot, called eddy currents, create ohmic heating directly in the pot itself [5]. Therefore, the only lost energy is that required to drive the circuitry controlling the magnetic field of the stove. Using induction heating, efficiencies as high as 90% or more can be realized [4].

1.2.1 Topologies

A number of converter topologies exist for efficiently producing the time varying magnetic field needed for induction heating. Two topologies are of particular interest in the field of induction

cooking: series resonant converters and series quasi-resonant converters. These topologies are of interest because, to the best of the author's knowledge, all existing induction cooking literature industry examine one of these two topologies.

The series resonant converter consists of a series resonant tank. This tank is fed by a voltage fed bridge, switching at the resonant frequency of the tank. The resonant frequency of any resonant tank is given by the equation in Figure 1-1. By driving the tank at its resonant frequency, large resonant currents are induced, which in turn are responsible for heating the cookware. Additionally, the power devices are inherently soft switched with this control mechanism. The driving bridge can either be a half bridge with two power devices (as shown in Figure 1-2) or full bridge with four devices.

$$f_0 = \frac{\omega_0}{2\pi} = \frac{1}{2\pi\sqrt{LC}}.$$

1-1 Equation For the Resonant Frequency of an LC Tank

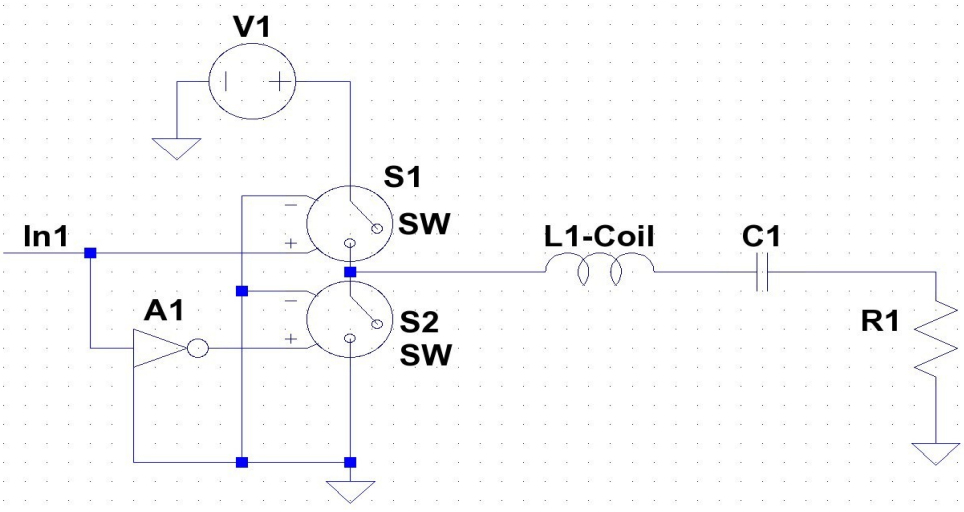

1-2 Schematic of a Series Resonant Converter with Half-bridge

The series quasi-resonant converter also uses a resonant tank, but just a single power

device. The device is turned on and the tank is allowed to resonate for one half cycle. At the zero crossing, the device is switched off. This alternate method also guarantees soft switching, but the controller must now pulse the power device to achieve heating.

1.2.2 Literature Review

Induction stoves, and the phenomenon of induction in general, have been studied extensively. A significant amount of scientific literature explores the phenomenon of eddy currents [5][6]. Practical uses include: eddy current testers, which use induction and the magnitude of eddy currents to check for cracks in frames of rockets, aircraft, and other high performance structures. Eddy current braking is used in high speed mag-lev rail and some electronic lifts. Induction heating, for either melting or heat treating metal is used extensively in industrial applications.

There is also a large body of work from academia and industry. There are a number of papers discussing quasi-resonant converter induction stoves, as well as fully resonant induction stoves. This is a very mature field, with a number of cutting edge designs presented each year from academia [7][8]. The literature from industry is diverse, including datasheets for induction stove specific ASICs, application notes discussing induction heating, and reference designs for stoves. These publications regularly achieve efficiencies in excess of 90% [4]. However, typcial efficiencies in industry fall into the 70-80% range [10][15].

However, a major shortcoming of the existing literature is the lack of other converter topologies explored. There are several academic works presenting designs of Class E amplifiers for induction stoves, but no other converter topologies have been thoroughly investigated for induction cooking.[1]

1 [9] claims to using using a parallel resonant tank; however, their topology is identical to a Class E amplifier and

their use of the term parallel resonant is at conflict with authorities on the subject [12].

1.3 Commercial Products

Several commercial products were examined to determine what topologies were popular in practice and to explore existing solutions to induction cooking.

1.3.1 Fabiano Stove

The Fabiano stove is a cheap, 220V single burner induction stove sold in India. It uses a quasi-resonant topology with a single power device and a 27kHz switching frequency. An approximate circuit diagram is reproduced in Figure 1-3. Pictures of the stove PCB are presented in Appendix A.

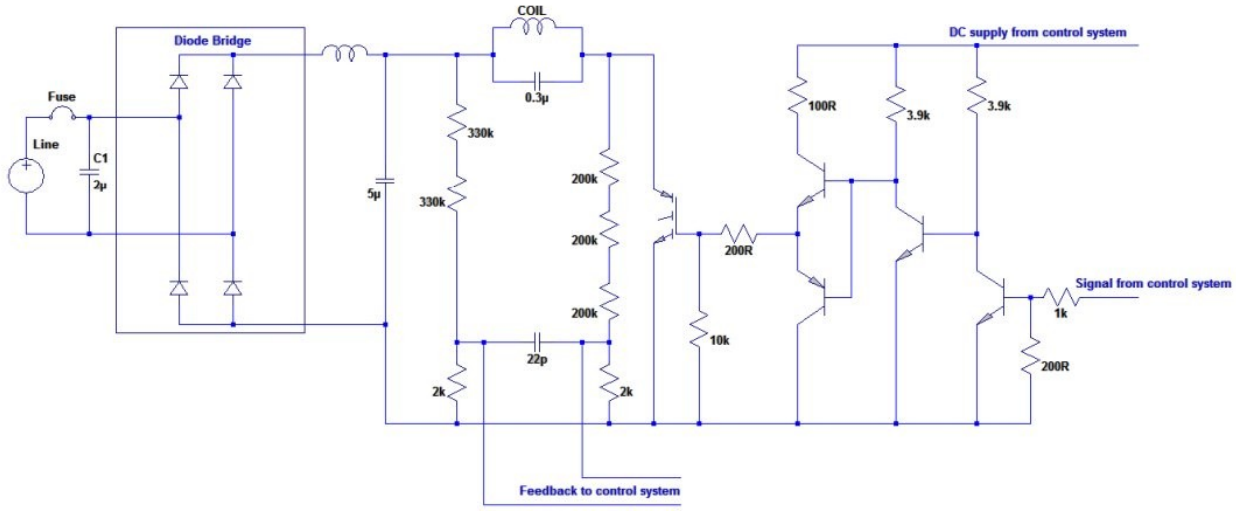

1-3 Schematic of the Fabiano brand stove with Quasi-Resonant Topology

1.3.2 Phillips Stove

The Phillips stove is another cheap induction stove sold in India. It also uses a quasi-resonant topology with a single IGBT and a 30kHz switching frequency. A close-up of the coil is included in Figure 1-4. Note the many strands of twisted conductors forming the “wire” in the coil. This is

to reduce skin effect and will be discussed more in Chapter 3. Pictures of the stove and its PCB can be found in Appendix A.

1-4 Depiction of Wound Coil in Phillips Stove

1.3.3 CookTek Stove

The CookTek is a high-powered industrial model sold in America. It uses a resonant half-bridge with 4 power devices (2 in parallel for each leg of the bridge) and operates at 25kHz. The PCB of the CookTek stove can be seen in Figure 1-5.

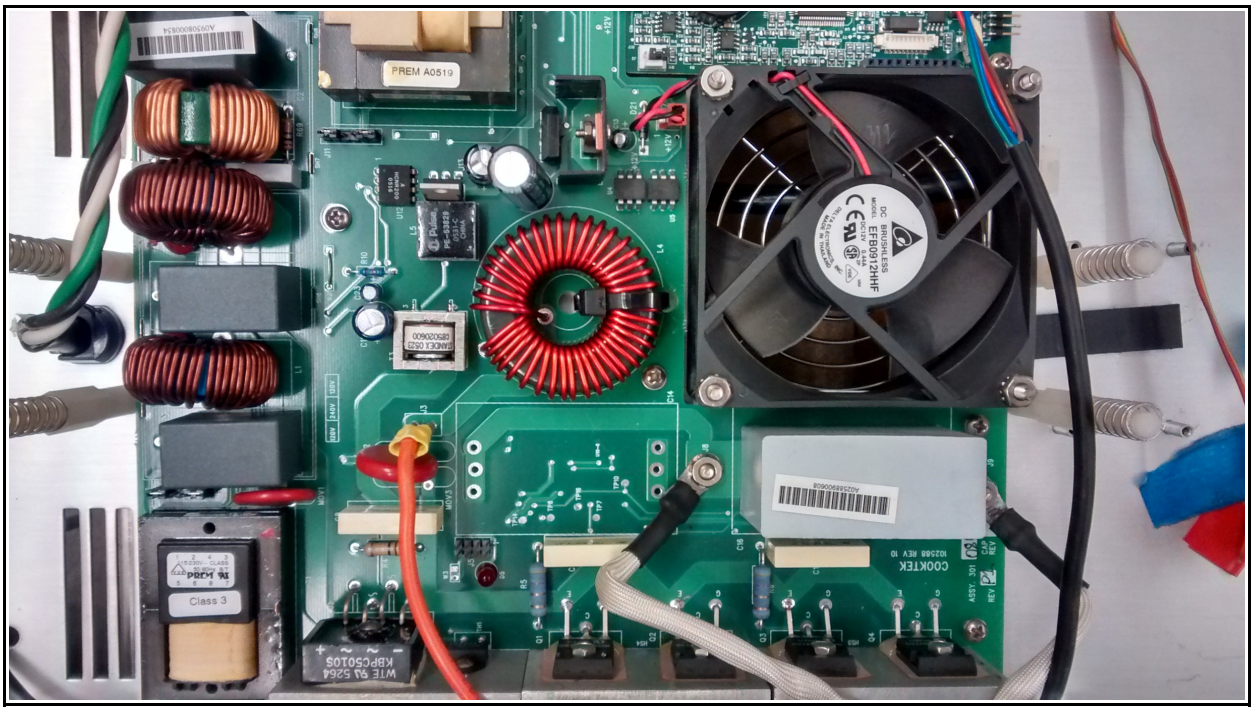

1-5 Depiction of PCB for CookTek brand stove with Series Resonant Topology

1.4 Limitations and Disadvantages of Existing Commercial Stoves

Existing commercial stoves have a disadvantages, especially in the context of use in developing areas. First off, although high efficiencies of 90% are well within grasp, many commercial offerings don't even reach 80% efficiency, likely because they were designed in countries with cheap, reliable mains power [10].

Furthermore, no existing stoves have built in mechanisms of dealing with brown-outs or black-outs. If a family relied on an induction stove in one of many cities in the whole without high quality electricity, they would be unable to cook their meals on a regular basis.

Additionally, no existing stoves have the ability to run off low voltage inputs. This is key to the strategy we present in Chapter 3 for dealing with the above situation.

Finally, commercial stoves are simply over-designed for most users in developing areas. They don't need the cooking power of a restaurant in a busy metropolis; they need to cook a little bit of rice for their daily meal. An induction stove designed for those people can take advantage of their lower power demands to provide them with features more in line with their lifestyle, such as a cheaper or more efficient stove.

Chapter Two

MIT Induction Stove System Design

2.1 Challenges

Developing countries and rural areas in developed countries present unique challenges to the design of any electric stove. The largest hurdle to overcome is the lack of readily available and reliable electric power. Consider India as an example. Many areas outside of the city have access to 220VAC wall outlets. However, they experience frequent power outages, interruptions, and poor power power quality [1]. Further outside the city in rural areas there may be no grid connection whatsoever. For electricity, these areas might rely on small solar installations, or town size “micro-grids”. Finally, any solution must be relatively low cost, or it will not be adopted.

These challenges are not adequately met by available electric stoves. Resistive element electric stoves suffer from low efficiencies. A single low efficiency stove may overwhelm a home solar installation, while a number of them drawing power at the same time may overwhelm a microgrid. Commercial induction stoves have high efficiencies, but even higher efficiencies are desirable. No existing solution is capable of coping with an intermittent grid connection. The proposed thesis project aims to address these shortcomings.

2.2 General Approach

Our approach addresses these problems by undertaking the design of a high efficiency induction stove powered by 24V DC. This represents a previously un-researched area as there are currently no commercial induction stoves or literature available in academia regarding induction stoves powered from a low voltage DC power source.

Such a stove would address the challenges highlighted in the previous section by utilizing a 24V DC power source. A 24V DC power supply could take several forms; a cheap and readily available form of a 24V DC supply is the connection of two car batteries in series. This addresses the problem in each of the three cases above. Instead of relying on flaky grid power, a home could instead charge two car batteries off the grid when power is available, and use the stored power for cooking in the event of a brownout or similar electrical interruption.

Furthermore, 24V is an extremely common output for solar installations, and one of only a few standardized output voltages for photovoltaic panels. This makes it appropriate for direct integration with a roof top solar installation or solar-based microgrid [11] Traditionally, to hook up an electric appliance, such as an induction stove, an inverter is connected to the solar battery to produce mains AC voltages. This step is usually at most 90% efficient, and frequently significantly less. Then the stove internally must rectify the AC voltage back to DC to use it, again with a loss of efficiency. Figure 2-1 shows a conventional approach, with losses at each step.

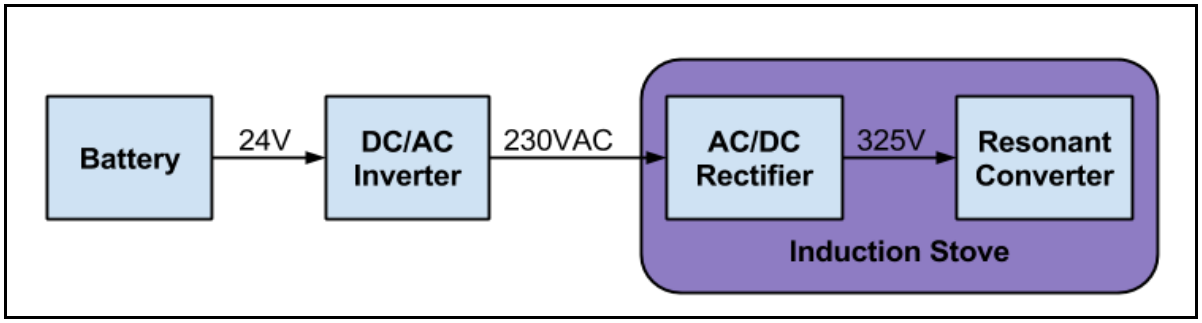

2-1 Block Diagram of Conventional Approach for Powering an Induction Stove from a Battery

By feeding our stove directly off the battery, we eliminate the inefficiencies associated with converting solar energy to AC for compatibility with appliances and then back to DC in the stove itself. Eliminating these steps could cut the wasted power of an induction stove in half. Figure 2-2 shows our approach for comparison.

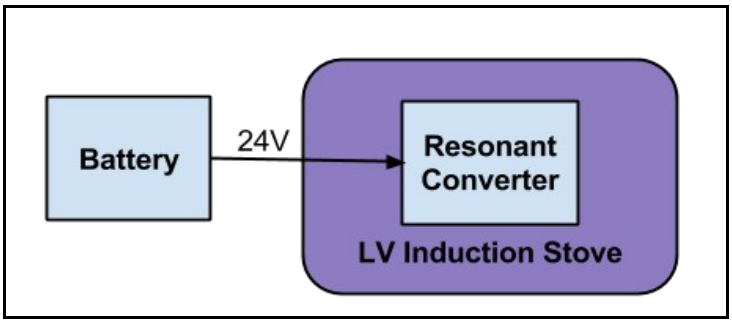

2-2 Block Diagram of MIT Induction Stove Approach for Battery Powered Induction Stove

2.3 System Components

Our design consists of 3 major components: the converter board, the control board, and the software to control it. The converter board contains the gate drivers, resonant tank, power devices, and feedback circuitry. The control board contain the microcontroller, as well as miscellaneous I/O and signal conditioning components. The software run on the control board and is responsible for the logic driving the switches of the converter board.

This paper focuses on the design of the resonant converter and the converter board. However, the software is intimately linked to the design and operation of the converter and control logic which resides in software will also be discussed.

2.4 Converter Topology

The topology that most suites our approach described above is not one of the conventional topologies used for induction cooking. Instead of using a series resonant, series quasi-resonant, or class E inverter, we choose to explore the current-fed parallel resonant converter. This converter has some use in industrial induction heating applications, but there is no prior information available about this topology's use in induction cooking. The rationale behind this decision, as well as the complications it produces will be detailed in the following chapter. Figure 2-3 shows an example of this topology.

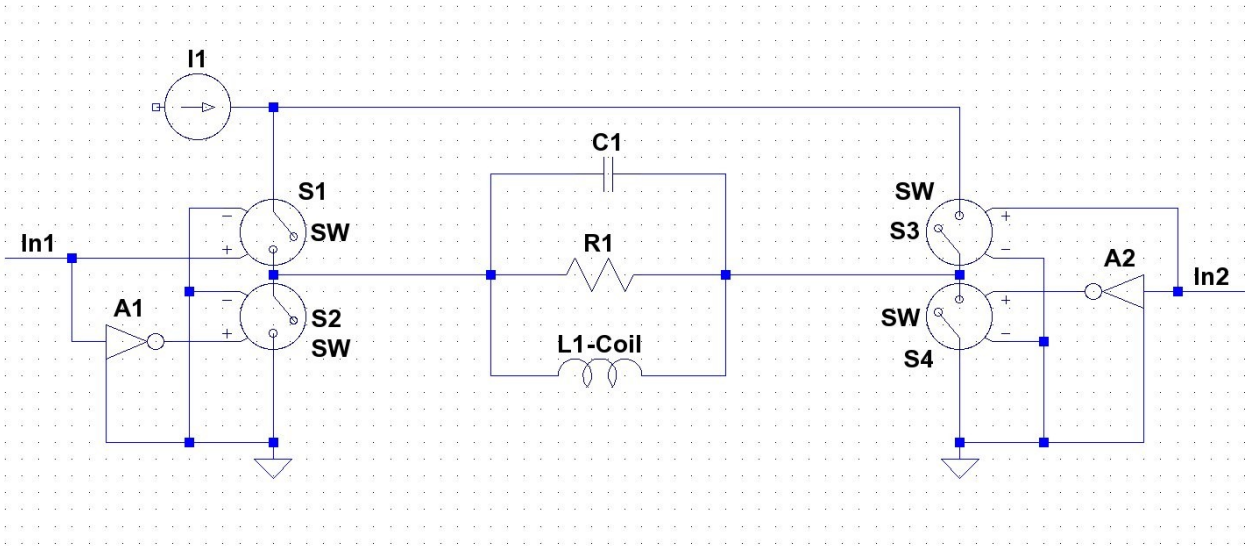

2-3 Conceptual Schematic of a Current-Fed Parallel Resonant Converter

2.5 Scope of Thesis

The purpose of this Thesis is to explore the design of an induction stove appropriate for use in developing areas. Included in the scope is an examination of existing methodologies and the proposal of a new solution. The dynamics of the design will be thoroughly detailed and

discussed. Additionally, simulations have been performed as needed to verify system behavior. However, this Thesis does not intend nor purport to provide an optimal implementation. Instead, the implementation presented will be a proof of concept. It will become the ground work for future research and have the ability to be easily scaled toward fully operable, practical designs.

Chapter Three

Induction Stove Converter Design

3.1 Basic Physics of Induction Heating

The primary sources of heat for cooking in the developing world are wood or fossil fuel derived products. The research into this field has produced an ISO standard for comparative testing of the effectiveness, efficiency, and emissions of stoves. This standard is referred to as the “Water Boil Test” [3]. The water boil test is carried out in a controlled environment with a precise set of conditions, and data is taken as a stove boils 3L of water in a pot.

Investigating what power is needed to boil 3L of water provides useful metric for designing a new induction stove. The energy needed to heat water from room temperature (~30C) to boiling (100C) is a function of the specific heat and heat capacity of water. For a 70C rise in temperature, this corresponds to about 0.25 kWh for 3L of water. If we consider 3L of boiling water adequate for cooking a family meal, we can see this provides a bounds on the system. 50 Watts is clearly far too low, as bringing 3L to a boil would take over 5 hours. On the other hand, people in the developing world don't need 3kW power output like restaurants in New York City demand. Therefore, the system design will aim at providing between a few hundred Watts (typical of a rice cooker) and up to 1 kW (a low end commercial induction stove).

3.1.1 Eddy Currents

Eddy currents are the primary mechanism by which heating occurs in induction stoves. The time varying magnetic fields induce currents in the pot proportional to the magnetic field intensity. These currents undergo ohmic losses due to the resistivity of the pot. Therefore, the loss is a function of both the pot resistivity and the coil configuration and current.

The pot / coil combination can be modeled as a transformer as in Figure 3-1. The coil inductance is then the magnetizing inductance, and the eddy current loss can be modeled as a resistor Z_L on the secondary. However, the turns ratio and effective resistance are both non-linear functions of the physical pot, its contents, the resonant frequency, and the magnetic field coupling between the coil and the pot.

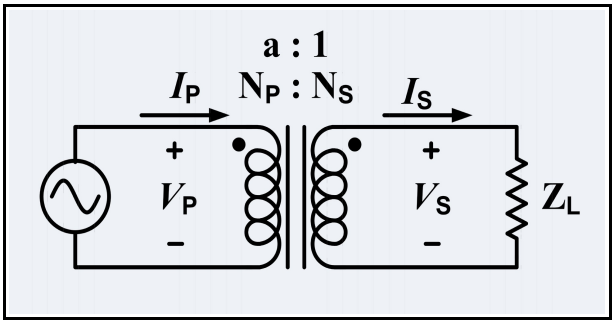

3-1 Model of Coil / Pot as a Transformer and Resistor

3.1.2 Hysteresis Loss

There is an additional loss (heating) mechanism in ferromagnetic materials called hysteresis loss. This loss can be thought of as energy needed to flip the magnetic dipoles in the ferromagnetic material and contributes a significant, but not overwhelming, percentage of the heat generated in

an induction stove [5].

3.1.3 Skin Effect

Skin effect refers to the tendency of high frequency currents to flow on the surface of conductors. The current density decreases exponentially with distance from the conductor's surface. The "skin depth" is the distance from the surface at which the current has followed to 1/e of the total current. The equation that governs skin depth is shown in Figure 3-2.

$$\delta = \sqrt{\frac{2\rho}{\omega\mu_r\mu_0}}.$$

3-2 Equation for Skin Depth

In induction heating, the skin effect produces a favorable outcome for heating a pot. As frequency increases, the effective resistance of the pot increases with the square root of frequency. It should also be noted that the skin depth is much larger in non-magnetic materials (i.e. materials with lower relative magnetic permeability) and therefore non-magnetic materials are not suitable for induction heating. Figure 3-3 shows the skin depth of various materials vs. frequency.

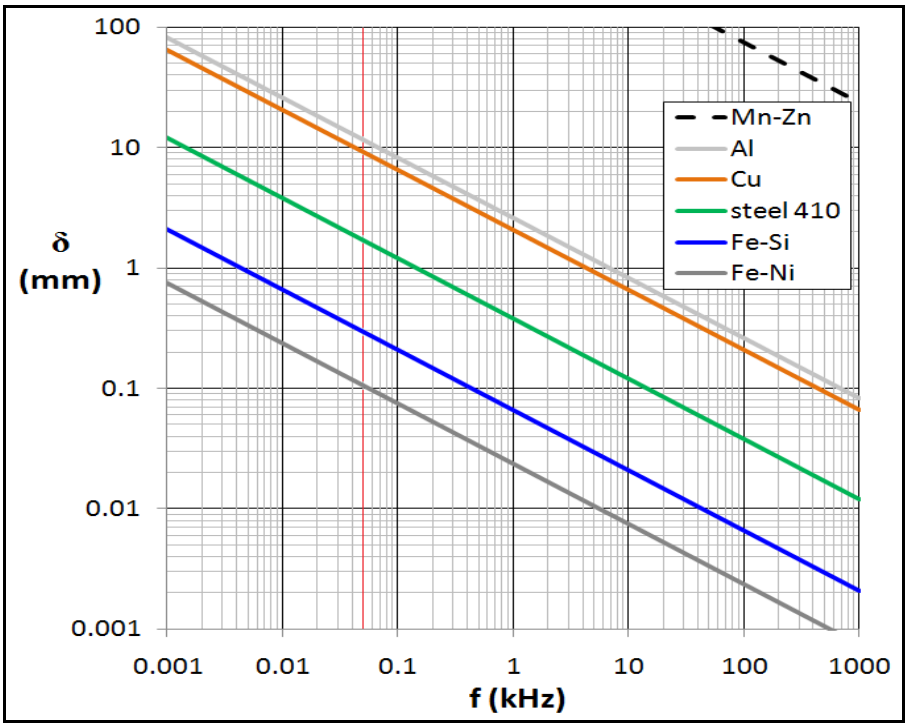

3-3 Graph of Skin Depth vs Frequency for Different Materials

3.1.4 Coil Physics

In essence, the goal of the induction stove is to produce as large of a magnetic field as possible. The magnetic field produced is a function of the coil geometry, as well as ampere-turns in the coil. The coil geometry is ideally a “pancake” coil for the purposes of an induction stove [14]. However, a helical coil will work as well.

The magnetic field is directly proportional to ampere-turns. However, simply increasing the number of turns is not always possible due to the dynamics of the converter. For instance, inductance is proportional to turns squared. Inductance also affects the resonant frequency so it is constrained by the other parameters of the system.

Finally, coils also experience ohmic loss exacerbated by skin effect. In this case, skin

effect hurts efficiency since we are attempting to heat the pot and not the coil! Furthermore, the more turns in the coil, the longer the conduction path will be. This translates to higher losses in the coil when additional turns are added.

3.2 Topology Selection

The overwhelming majority of existing induction stoves use either a series resonant or series quasi-resonant design. However, as shown in Figure 2-1, these stoves typically operate with their converter stages fed by a large DC voltage. In contrast, our design operates with a low voltage DC input as shown in Figure 2-2. One simple solution would be to boost the input voltage, but then we are adding an additional stage with loss, similar to the conventional design.

Operating a traditional design at a lower voltage is simply not feasible. All other parameters being equal, the input voltage is directly proportional to output power. This is because the minimum impedance of the coil / resonant capacitor network is essentially fixed. It's something of a Catch 22. Building a high Q induction stove to increase resonating current is simply not possible because you *want* maximum damping. That damping is power transmitted to your load.

As we can see from the discussion of the physics of the system, if we wish to increase the power output, we need to increase the ampere-turns in the coil, the frequency, or both and at the same time, to maintain efficiency, we wish to minimize loss.

Increasing only frequency isn't viable. The resistance only scales with the square root of of frequency. We are operating at ~10x lower input voltage, which means we'd need to operate at 100x the speed. This is impractical. Traditional devices and topologies are already near their

limit at 30kHz and switching losses and coil losses would skyrocket.

As stated above, simply increasing the turns in the inductor is not a viable option due to system constraints. Counter-intuitively, increasing the turns actually reduces the ampere-turns because for every time the turns are doubled, the current flowing is decreased by a factor of 4. This can be seen from the equation for inductance of a coil in Figure 3-4 and the conservation of energy equation in Figure 3-5. To keep the same switching frequency, we'd need to decrease the capacitance by an equal amount. Therefore, we must have higher currents and switching speeds to make up for our low input voltage.

$$L = \mu_0 \frac{N^2 A}{l}.$$

3-4 Equation for Inductance of a Coil

$$\frac{I_0}{V_0} = \sqrt{\frac{C}{L}}$$

3-5 Equation for Peak Current as a Function of L, C, and Peak Voltage

In a series resonant converter, the power devices must carry the resonant current and block the resonant voltage. This equates to large, slow devices and large conduction losses. Our solution instead is to adopt a topology from industrial induction heating: the full-bridge parallel resonant converter. A generalized view of this architecture is presented in Figure 2-3.

The parallel resonant converter has little or no presence in available literature on induction cooking. A significant advantage this topology has is that resonant current stays entirely in the resonant tank. The power devices need only carry the current actually delivered to the load. For a 24V source providing 1kW of heating, that's a maximum of ~40 amperes. A major complication is that a parallel resonant circuit must be current-fed to resonate. We believe the

lack of existing research into this topology is due to the difficultly of dealing with a current-fed architecture, combined with the fact that most induction stoves are operated off of high voltages to begin with.

3.3 Operation Frequency

The operating frequency is one of the primary system parameters. It has a large effect on performance. As operating frequency goes up, the skin depth in the pot decreases, thus increasing loss in the pot or, equivalently, the heating effect. This means higher operating frequency is highly desirable.

As frequency increases, switching losses in the power devices increase, as do losses in the coil from skin effect. This can be significant, but it is usually outweighed by the efficiency gains from operating at higher frequencies. The practical limitation in switching frequency is usually the maximum switching frequency of the power device. For IGBTs, this is typically in the tens of kHz. For MOSFETs, this can be in the MHz range.

Our design operates at 50 kHz. This is approximately twice the switching frequency of the commercial designs examined. Additionally, the design presented has the capabilities to easily scale to 100kHz and beyond. Lower device stresses due to our parallel resonant topology allow faster device switching than conventional designs. More detail is provided in section 3.5.

3.4 Ideal Current Source vs. Voltage Source & Inductor

The major complication with a practical implementation is that ideal current sources are not readily available and are hard to emulate. Our design approximates an ideal current source with a

large inductor in series with our battery (denoted Vdd) which is a near ideal voltage source. A practical implementation of Figure 3-6 is presented in Figure 3-6. Figure 3-6 contains additional circuitry and calculated values from further sections; this schematic was used for simulation results presented, unless otherwise stated.

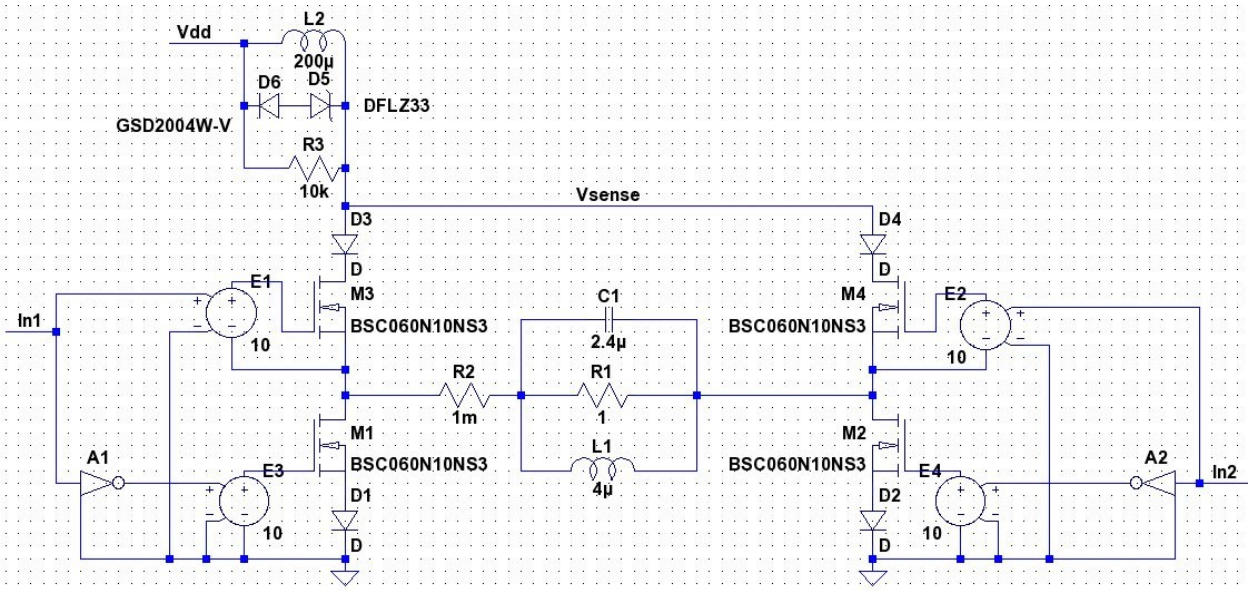

3-6 Practical Implementation of a Parallel Resonant Converter

This method in practice presents two problems. First, when the devices are turned off, the inductor will continue to conduct into a high impedance node, which results in a voltage spike. D5, D6, and R3 were added to limit and damp the voltage spike.

Second, we cannot directly control the current produced by our approximate current source. Instead, the current produced is a function of the input voltage and the system dynamics. So what constraints does the inductor impose? Steady state conditions mandate that the volt-seconds across the inductor in one cycle must be equal. Therefore, the average voltage on right side must equal the input voltage. *This is an extremely important result for the design of this converter.* A ringing resonator switched perfectly at the zero voltage crossing (i.e. a 50% duty

cycle) will result in the right side of L2 seeing a rectified sine wave. The average value of a rectified sine wave is 2/π times the peak voltage. Or, equivalently, *the peak voltage in the resonator can be no more than π/2 times the input voltage Vdd* when switched at 50% duty cycle on the zero voltage crossing. This equation is represented in Figure 3-7. This means that the peak voltage during operation off a 24V source is less than 40V.

$$V_{sense0} = (\frac{\pi}{2}) \cdot V_{dd}$$

3-7 Equation Governing Peak Voltage on V_{sense}

An equally important result to understand is that the peak voltage increases the further we operate off resonance. If we switch slower than resonance, V_{sense} goes negative for part of the cycle, and therefore the peak voltage must rise to compensate. If we operate faster than resonance, the waveform shape gradually changes from a sinusoid to a sawtooth. This can be explained by the small angle approximation: the sooner we switch in the resonant half-period, the smaller the argument to the sine is. Furthermore, since switching flips the polarity V_{sense} sees, the sawtooth starts negative, thus increasing peak voltages. Overall peak voltage reaches its maximum at ~4x Vdd.

3.5 Power Devices

3.5.1 IGBT vs. FET

Traditional designs typically use IGBTs as switching devices. These devices have the advantage of being able to tolerate large currents, high voltages, and block reverse conduction. However, the maximum operating frequency is limited to the kHz range and conduction losses are typically

larger at low voltages than FETs.

MOSFETs are typically eschewed by induction cookers because they can't tolerate the extreme voltages and currents present in series resonant designs. They offer much higher switching speeds and lower conduction loss at low currents. A significant disadvantage for this application is that they do not block reverse conduction

However, our design limits voltages to less than 100V and currents to less than 40A. This is in stark contrast to series resonant converters, that may require the components to withstand hundreds of volts and hundreds of amps. This allows us to get away with using MOSFETs as the switching devices, thus allowing extremely high switching frequencies.

We choose the IRFP4310P for all 4 switching devices. These are 100V N-channel MOSFETs with 6 mOhm $R_{ds(on)}$ and 170 nC total gate charge. Using all N-channel devices adds some complexity, but the superior performance of NFETs outweighs the disadvantages.

3.5.2 Zero Voltage Switching (ZVS)

A major advantage of any resonant converter topology is it inherently allows soft switching. In series resonant converters, it allows for Zero Current Switching (ZCS). Parallel converters, on the other hand, allow for ZVS. This reduces switching losses to effectively negligible levels.

3.5.3 Power Diodes

These are only needed when using MOSFETs as the switching device. We selected APT30S20BG Schottky diodes, which have 850mV forward voltage, minimal reverse recovery charge, and 45A current rating. With a Junction to Ambient thermal resistance of 40C/W and a

maximum operating temperature of 150C, these devices will require a heat sink.

3.6 Resonant Tank Design

The resonant tank's behavior is governed by 3 major equations. The maximum voltage equation (Figure 3-7), the resonant frequency equation (Figure 1-1), and conservation of energy (Figure 3-5).

3.6.1 Capacitors

Given that we have a fixed input voltage, the conservation of energy equations imply that we'd like as large a capacitor as possible. However, there are limits to the performance of readily available capacitors at high frequencies. In particular, many capacitors need significant voltage derating at high frequencies. We chose polypropylene capacitors from the TDK MKP series, part number B32656T. These were selected for their 1250V voltage rating and low ESR. The voltage derating curve is shown in Figure 3-8. These capacitors are the major limiting factor preventing the switching frequency from being increased.

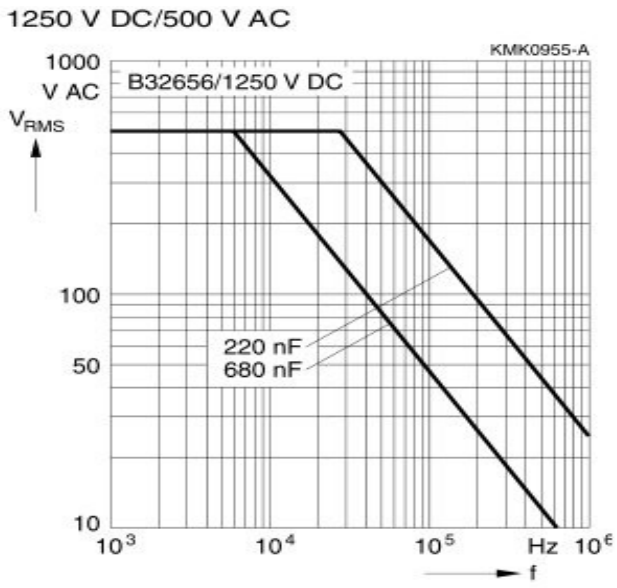

3-8 Voltage Derating Curve for Capacitors vs. Frequency [17]

Another point of concern is that if the tank capacitor cannot store enough energy, the system will be overdamped and will fail to resonate completely. This results in loss of soft switching. A simulation of a converter with a capacitor too small for the power output can be found in Figure 3-9; notice how the voltage Vsense approaches 0 exponentially before being switched instead of being a full sine wave.

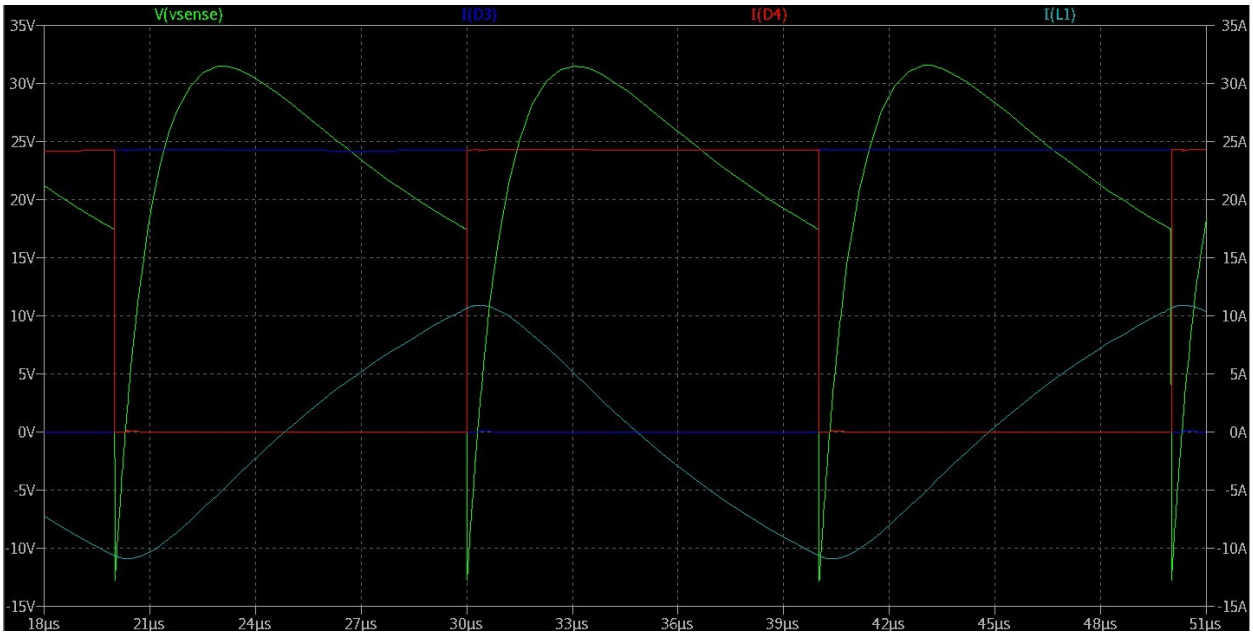

3-9 Simulation of Resonant Tank with a Small Tank Capacitor

The capacitor value is chosen to be 2.4uF, or 6 0.4uF capacitors in parallel. This is because 0.4uF are the largest capacitors readily available suitable for the high voltages and currents. 2.4uF provides sufficient energy storage while allowing a reasonable number of capacitors to be used.

3.6.2 Coil

If the switching frequency is fixed and the capacitor size is already chosen, the size of the inductor is completely constrained. In this case, the value must be 4uH for a 50kHz switching frequency. Coil inductance will always be approximate since the presence of a pot will significantly alter the inductance. Therefore, it is not important to get exact numbers. Fortunately, coils are easy to compare since all stove coils are air-core and 8-10 inches in diameter. This results in about 3 turns for a 4uH coil and 8 turns for a 30uH coil (typical). We choose a 3 turn

coil of 8 inches in diameter. This gives approximately 3.7uH of inductance in free space. To simplify construction & minimize cost, this coil is fabricated out of 0.25 inch copper tubing. Because of skin effect, tubing is actually a very sensible choice with little wasted material. Aluminum tubing would work equally well at the expense of slightly higher power dissipation.

It is important the coil has the appropriate number of ampere-turns for the heating power desired. Empirical evidence suggests that about 160 ampere-turns per kW is about right for 25kHz operation [15] For 500W operation at 50kHz, that would be about 60 ampere-turns. With a 3 turn coil, we would like to see around 20A peak. Simulations in Figure 3-10 show peaks just over 25A for 500W operation.

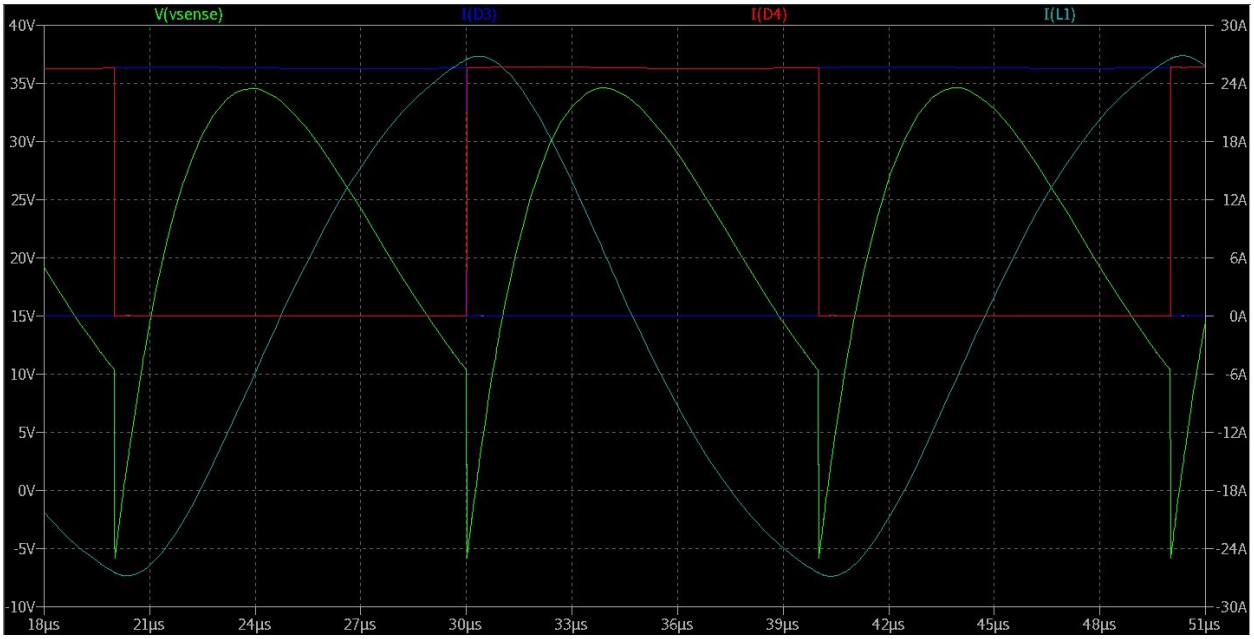

3-10 Simulation Showing Peak Resonant Current at 500W output

3.7 Gate Drivers

Gate driver chips must be able to turn on 100V MOSFETs within a fraction of the resonant period. If we want to spend less than 5% of time switching at 50kHz, we must switch faster than

500ns. Most 100V MOSFET gates have less than 200nC total gate charge. This means we should be looking at gate drivers that can source and sink at least 400mA.

We chose the STM L6384. These gate drivers also provide deadtime control to prevent shoot through and are capable of driving a high side N-channel FET are highly desirable.

Chapter Four

Implementation & Performance

4.1 Efficiency Analysis

In an attempt to estimate the efficiency of the overall system, power dissipation of the most important components was calculated assuming a 500W output operating point. These estimates are supported by simulations of the system.

4.1.1 FET Switching Losses

Switching losses in MOSFETs can be broken into two primary components. First, the conduction losses occurring when switching. If the FET is conducting while being switched, the losses will be equal to the area under both curves in Figure 4-1. However, this can be avoided by soft switching. The resonant converter controller is designed to begin switching the devices just before the zero voltage crossing. This reduces conduction losses while switching to negligible levels.

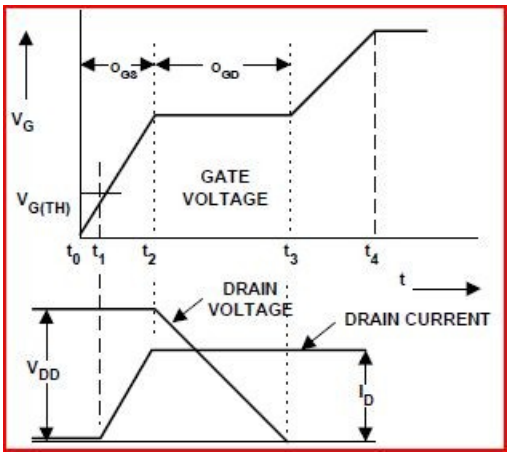

4-1 Diagram of Gate Charging [18]

Second, energy is lost charging and discharging the gate capacitance every cycle. The IRFP4310Z has a gate capacitance of 8nF at 15V. Switching at twice a cycle at 50kHz gives 100mW dissipation per device.

4.1.2 FET Conduction Losses

Conduction losses are ohmic losses from channel resistance while the device is conducting. The IRFP4310Z has a max $R_{ds(on)}$ of 6 mOhm. With each device conducting 25A half the time, the power dissipation per device is 1.6 W. This otherwise conservative estimate could almost double if the device is operating near it's maximum temperature.

4.1.3 Diode Conduction Losses

Diode losses are simply forward voltage time current. Schottky diodes have no reverse recovery charge to dissipate. The power diodes conduct half of the time at 25A, which results in 10 W dissipation per device. The diode forward voltage drops by more than 10% at its maximum temperature from room temperature, making this estimate fairly pessimistic.

4.1.4 Coil Losses

The coil will also exhibit conduction losses. The coil length is ~1m: just over 60cm for the coil, and 20 cm for each leg. At 50kHz, the skin depth of copper according to Figure 3-3 is 0.3mm. The resistance of a 0.25 inch tube is therefore ~3mOhm. A 25A peak sinusoid as in the simulation in Figure 3-10 results in approximately 1W of dissipation. Replacing the copper tubing with aluminum tubing would add < 1 W of dissipation.

4.1.5 Filter Inductor Losses

The filter inductor conducts 25A DC with a resistance of 7mOhm. This equals 4W power dissipation.

4.1.6 Efficiency Calculations

The total losses are ~55 Watts. Dissipation by device is as follows: 40W in the diodes, 8W in the FETs, 4W in the filter inductor and 1W in the coil. This results in the system consuming 555W at 500W output, resulting in an efficiency of just over 90%. Of course, these are just estimates, and do not include the contributions of the control circuitry. However, one should expect a real life efficiency of about 90% operating at 500W for this design.

4.2 Printed Circuit Board Implementation

The design was implemented on a printed circuit board in Figure 4-2. This is a 2-layer, 5.5 x 6.5 inch PCB containing the parallel resonant converter power devices, feedback circuitry, and gate

driver circuitry. The schematics are presented in Figure 4-3 and Figure 4-4. Additional pictures can be found in Appendix A.

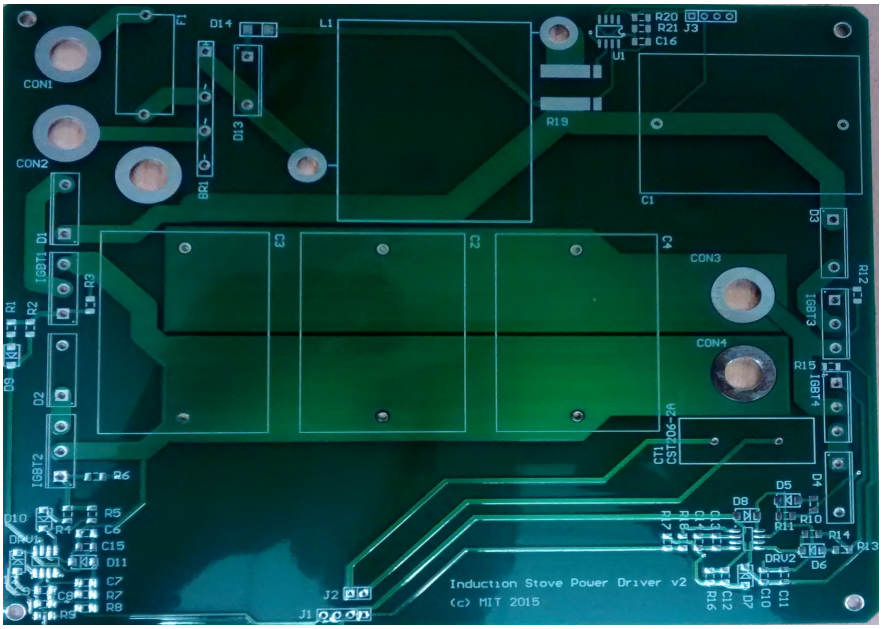

4-2 Depiction of Parallel Resonant Converter Printed Circuit Board

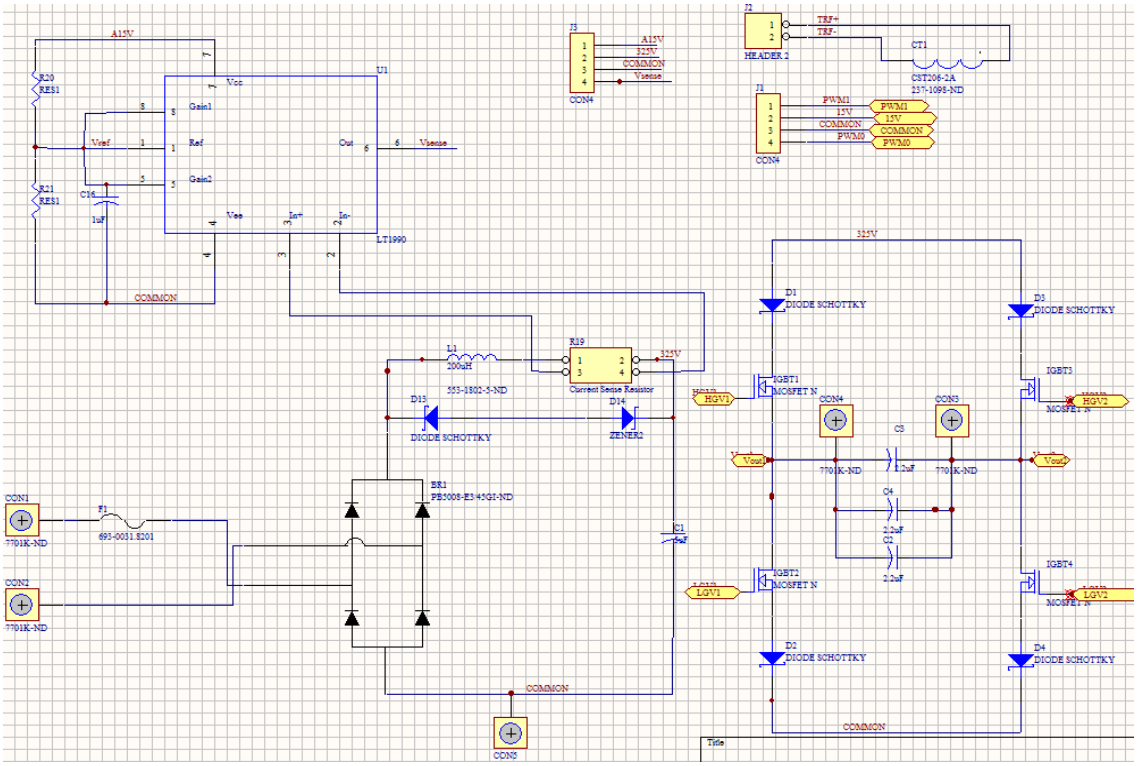

4-3 Schematic of Resonant Converter

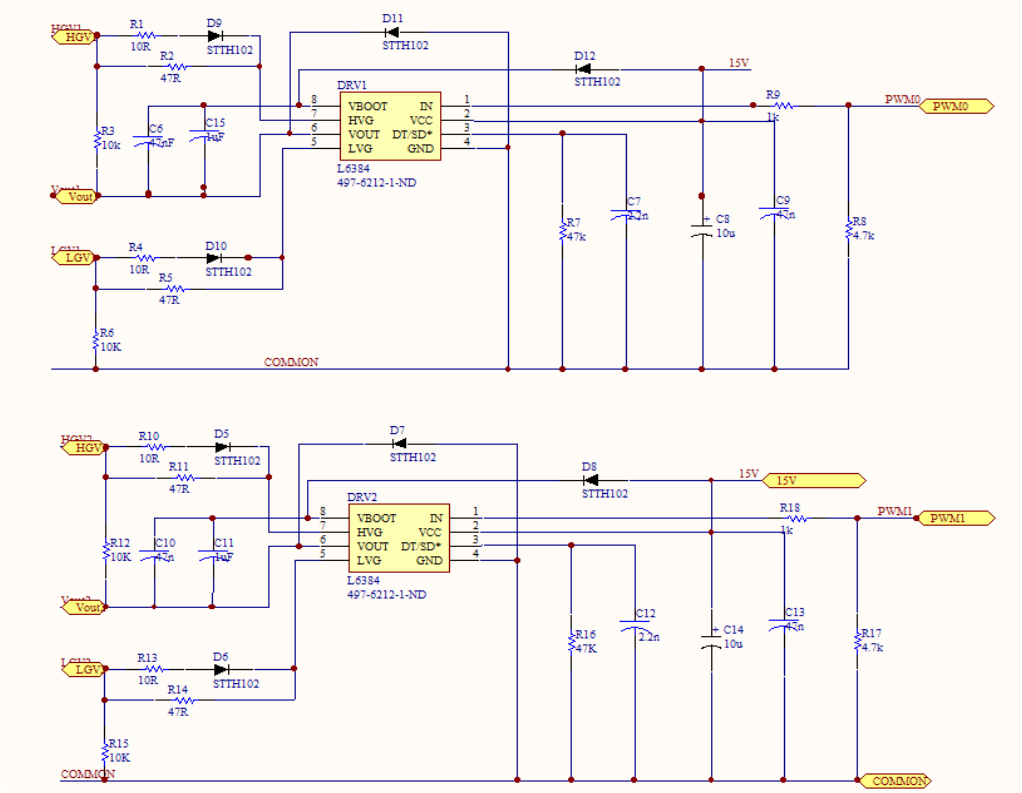

4-4 Schematic of Gate Driver

Chapter Five

Summary and Future Work

5.1 Summary

This thesis has investigated the design of an induction stove for the developing world and presented a novel solution to the problem. The design incorporates the following innovations:

- Low voltage operation for use with batteries
- Parallel resonant conversion for efficient power transfer
- MOSFETs instead of IGBTs to achieve higher frequencies and lower costs
- Ability to operate with a cheap copper or aluminum tube as the resonant coil
- Twice the switching frequency of commercial designs, with the ability to scale higher
- State of the art efficiency compared to other induction stoves. Massive efficiency gains when used in a battery system by eliminating the DC/AC inverter

This design successfully utilizes a converter topology from other applications to create a unique contribution to the field of induction stoves. This enabled the design of the first efficient, low input voltage induction stove. When integrated with a car battery or solar micro-grid system, this system has the ability to deliver massive efficiency improvements and never before seen reliability in the face of low quality mains power.

5.2 Future Work

This work only touches the surface of what is possible with this topology. Three main areas present the lowest hanging fruit for the future evolution of this design: operating frequency, coil design, and control strategy.

First and foremost, higher operating frequencies are possible with minimal changes to the resonant tank and driver circuitry. The design was specifically chosen to allow much higher operating frequencies. The current operating frequency, despite being nearly double most induction stoves', was chosen conservatively for this proof of concept implementation. Higher operating frequencies could lead to more efficient, compact, and affordable solutions.

Second, the coil design presented was the simplest coil design capable of working with this design. There is a significant potential for innovation in the design of the resonant coil.

Finally, the firmware for control was designed for maximum simplicity to reduce errors. This means there are a number of options to improve of the status quo. More feedback signals are available to the microprocessor than are used in the control loop. These additional signals could allow for interesting algorithms. Additionally, the full bridge switch configuration allows for many control schemes [13]. Additional work on the controls could result in more effective heat control.

Appendix A – Additional Figures

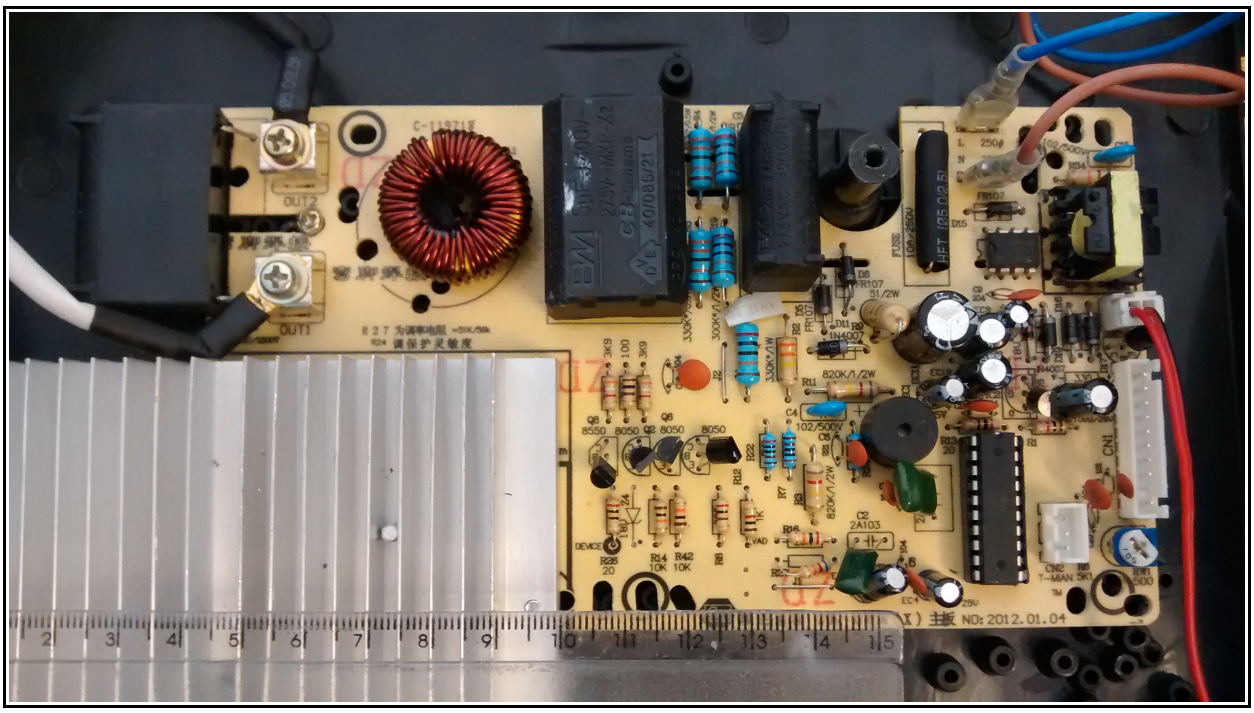

A-1 Depiction of Fabiano Brand Stove PCB

A-2 Depiction of Pot on Top of Phillips Stove

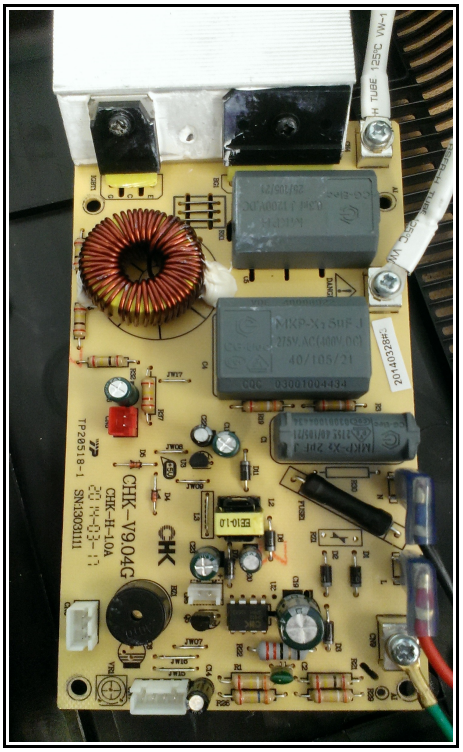

A-3 Depiction of Phillips Stove PCB

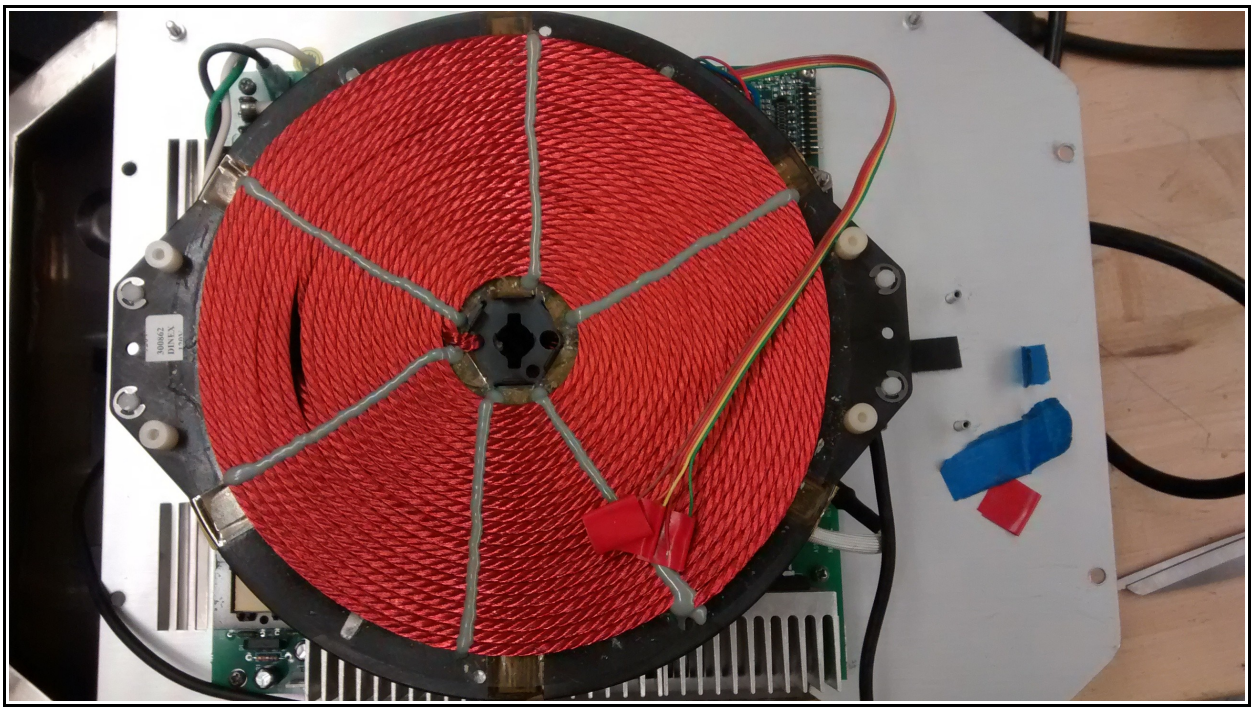

A-4 Depiction of CookTek Stove Coil

Appendix B – Control Code Excerpts

Code for stove-v1-0.c:

```
     1      #include "stove.h"
     2
     3      #define VDD 20 //Input voltage to power stage in volts
     4      #define SWITCH_VOLTAGE 20
     5      #define HYS_VOLTAGE 40
     6
     7      void init(void);
     8      void initInt(void);
     9
```

Omitted lines 10-21

```
    22
    23      int main(void)
    24{
    25            uint16_t adcValue;
    26            uint16_t i;
    27
    28            init();
    29
    30            ledBlink();
    31
    32            PMIC.CTRL |= PMIC_LOLVLEN_bm;
    33
    34            // Set up interrupts for pot detect and FET switching
    35            initInt();
    36            sei();
    37      while(1) {
    38                  //Do nothing; wait for interrupts
    39                  if (secFlag)
    40                  {
    41                  secFlag = false;
    42                        tglPin(LED1);
    43                  }
    44      }
    45
    46
    47      /*Old main loop */
```

Omitted lines 48-84

```
    85
    86            return 1;
    87}
    88
    89      void initInt(void)
    90      {
    91
    92            /*Channel 0: for current reading / pot detection*/
    93            ADCA.CTRLB = ADC_RESOLUTION_8BIT_gc | ADC_FREERUN_bm;
```

```
 94
 95             ADCA.REFCTRL = ADC_REFSEL_INTVCC_gc | ADC_BANDGAP_bm;
 96
 97             ADCA.PRESCALER = ADC_PRESCALER_DIV4_gc;
 98
 99           ADCA.CH0.CTRL = ADC_CH_INPUTMODE_SINGLEENDED_gc;
100
101       ADCA.CH0.MUXCTRL = ADCA_TEMP;
102
103       ADCA.CH0.INTCTRL = ADC_CH_INTMODE_COMPLETE_gc |
ADC_CH_INTLVL_LO_gc;
104
105
106       /* Channel 1: voltage sensing / zvs triggering*/
107
108     ADCA.CH1.CTRL = ADC_CH_INPUTMODE_SINGLEENDED_gc;
109
110       ADCA.CH1.MUXCTRL = ADCA_CURRENT;
111
112       ADCA.CH1.INTCTRL = ADC_CH_INTMODE_COMPLETE_gc |
ADC_CH_INTLVL_LO_gc;
113
114
115
116       ADCA.CTRLA |= ADC_ENABLE_bm; // start free running ADC
117
118}
119
120       void init(void)
121{
122             uint8_t baudrate;
123
124#if BAUD_INIT == 9600
125             baudrate = BAUD_9600;
126       #elif BAUD_INIT == 19200
127       baudrate = BAUD_19200;
128       #elif BAUD_INIT == 38400
129             baudrate = BAUD_38400;
130       #elif BAUD_INIT == 57600
131       baudrate = BAUD_57600;
132       #elif BAUD_INIT == 115200
133             baudrate = BAUD_115200;
134#endif
135
136             halInit();
137       eepromInit();
138             //    adcInit();
139             ftdiInit(baudrate);
140       commInit();
141
142       timerInit();
143       //    pwmInit(TC_PWM1, TC_PWM2);
144}
```

```
145
146ISR(ADCA_CH0_vect)
147{
148      static uint8_t potCounter = 0;
149
150            if(potDetect) { // in potDetect mode
151            if(potCounter == 0) {
152                        setPin(PWM1_PIN);
153                        clrPin(PWM2_PIN);
154
155                        if(ADCA.CH0.RESL > 50)
156                              potCounter++;
157
158                  } else {
159                        clrPin(PWM1_PIN);
160                  clrPin(PWM1_PIN);
161
162                  if((potCounter & 0x01)
163                     && ADCA.CH0.RESL < 50) // potCounter odd
164                        potCounter++;
165                  else if(!(potCounter & 0x01)
166                              && ADCA.CH0.RESL < 50) // potCounter even
167                        potCounter++;
168            }
169
170            if(potCounter > 10) {
171                  potDetect = false; // pot detected! Exit potDetect
mode!
172                  potCounter = 0;
173                  setPin(PWM1_PIN); // turn on the converter
174            }
175
176
177      }
178}
179
180ISR(ADCA_CH1_vect) { //In heating mode
181      static bool fallingEdge = false;
182
183      if(!potDetect) {
184            if(!fallingEdge && ADCA.CH1.RESL > (SWITCH_VOLTAGE +
HYS_VOLTAGE))
185                  fallingEdge = true;
186            else if(fallingEdge && ADCA.CH1.RESL < SWITCH_VOLTAGE) {
187                  tglPin(PWM1_PIN);
188                  tglPin(PWM2_PIN);
189                  fallingEdge = false;
190            }
191      } else {
192            fallingEdge = false;
193      }
194}
```

Code for timer.c:

```
 1      #include "timer.h"
 2
 3      volatile bool msecFlag = false;
 4      volatile bool secFlag = false;
 5      volatile bool potDetect = true;
 6
 7      void timerInit(void)
 8      {
 9            TC0_t *tmr = &TCD0;
10
11      hal_tmrSetClock(tmr, TC_CLKSEL_OFF_gc);
12
13            hal_tmrSetCounter(tmr, 0);
14
15            hal_tmrSetPeriod(tmr, 124);
16
17      // one tick is 1 ms for a 32MHz xtal
18      hal_tmrSetClock(tmr, TC_CLKSEL_DIV256_gc);
19
20            hal_tmrEnableOvfInterrupt(tmr);
21}
22
23      ISR(TCD0_OVF_vect)
24{
25            static uint16_t msecCounter = 0;
26
27      msecFlag = true;
28            if (++msecCounter > 999)
29            {
30                  msecCounter = 0;
31            secFlag = true;
32                  potDetect = true;
33            }
34      }
```

Bibliography

[1] United Nations Environment Programme, “UN Engages Banks to Light Up Rural India,” http://www.unep.org/Documents.Multilingual/Default.asp?DocumentID=504&ArticleID=5570&l=en, 2007

[2] Global Alliance for Clean Cookstoves, “Cookstove Fuels,” http://www.cleancookstoves.org/our-work/the-solutions/cookstove-fuels.html, 2014

[3] Global Alliance for Clean Cookstoves, “Guidelines and Standards,” http://www.cleancookstoves.org/our-work/standards-and-testing/guidelines-and-standards/, 2014

[4] ST Micoelectronics, “A single plate induction cooker with the ST7FLITE09Y0,” http://www.st.com/st-web-ui/static/active/en/resource/technical/document/application_note/CD00115561.pdf, 2009

[5] Agarwal, Paul D., "Eddy-current losses in solid and laminated iron," *American Institute of Electrical Engineers, Part I: Communication and Electronics, Transactions of the* , vol.78, no.2, pp.169,181, May 1959

[6] Dodd, C. V., “Some eddy-current problems and their integral solutions,” *Oakridge National Laboratories*, April 1969

[7] Llorente, S.; Monterde, F.; Burdio, J.M.; Acero, J., "A comparative study of resonant inverter topologies used in induction cookers," *Applied Power Electronics Conference and Exposition, 2002. APEC 2002. Seventeenth Annual IEEE* , vol.2, no., pp.1168,1174 vol.2, 2002

[8] Kumar, P.S.; Vishwanathan, N.; Murthy, B.K., "A full bridge resonant inverter with multiple loads for induction cooking application," *Energy Efficient Technologies for Sustainability (ICEETS), 2013 International Conference on* , vol., no., pp.119,124, 10-12 April 2013

[9] Leisten, J.M.; Hobson, L., "A parallel resonant power supply for induction cooking using a GTO," *Power Electronics and Variable-Speed Drives, 1991., Fourth International Conference on* , vol., no., pp.224,230, 17-19 Jul 1990

[10] Sweeney, M.; Dols, J.; Fortrnbury, B.; Sharp, F., “Induction Cooking Technology Design and Assessment,” *ACEEE Summer Study on Energy Efficiency in Buildings, 2014*

[11] Singh, Seema, “Solar Microgrids,” http://www2.technologyreview.com/article/427670/solar-microgrids/, *MIT Technology Review*, May/June 2012

[12] Kassakian, John G., “Principles of Power Electronics,” page 212, 1991

[13] Kassakian, John G., “Principles of Power Electronics,” page 222, 1991

[14] Zinn, S.; Semiatin, S. L., “Coil design and fabrication: basic design and modifications,” *Heat Treating*, vol.,no.,pp.32,41, June 1988

[15] On Semiconductor, “AND9166/D Induction Cooking,” http://www.onsemi.com/pub/Collateral/AND9166-D.PDF, Oct 2014

[16] On Semiconductor, “AND9201/D The Effect of Pan Material in an Induction Cooker,” www.onsemi.com/pub/Collateral/AND9201-D.PDF, Jan 2015

[17] “Metallized Polypropylene Film Capacitors (MKP) Series/Type: B32651 ... B32656 Datasheet,” EPCOS AG, Mar 2015

[18] “International Rectifier IRFP4310ZPbF Datasheet,” International Rectifier, Mar 2008